BILINGUAL PUBLISHING CO.
Pioneer of Global Academics Since 1984

Hydro Science & Marine Engineering
https://ojs.bilpublishing.com/index.php/hsme

ARTICLE

Adverse Impacts of Climate Change in Maharlou Lake Basin, Iran

Babak Zolghadr-Asli[1*] Siavash Behrooz-Koohenjani[2]

1. Teaching Assistant, Dept. of Irrigation & Reclamation Engineering, Faculty of Agricultural Engineering & Technology, College of Agriculture & Natural Resources, Univ. of Tehran, 3158777871 Karaj, Iran
2. Water Resources Research, Fars Regional Water Authority, Shiraz, Iran

ARTICLE INFO

Article history
Received: 2 December 2019
Accepted: 27 December 2019
Published Online: 31 December 2019

Keywords:
Climate change
Maharlou Lake Basin
CanESM2
IHACRES
Water resources

ABSTRACT

Climate change can alter the *status quo* of the world as we know today. Water resources may also be influenced by these plausible impacts. The common perception is that these changes may exacerbate the situation of water resources in arid and semi-arid regions, such as the Middle-East, which are experiencing mild to severe water stress due to limited water availability and growing water demands. In that spirit, this study aims to investigate the possible impacts of climate change on surface water in Maharlou Lake basin, Iran. Reportedly, this basin has already shown some symptoms of the water-related crisis, which highlights the importance of conducting climate change studies in this region. The CansESM2 model was employed to predict the basin's climatic response under various climate change scenarios. The hydrologic response of the basin was, then, simulated using IHACRES. The results have demonstrated a 4% decrease in average annual rainfall, a 2% increase in average annual temperature, and, finally, a 24% decrease in average annual streamflow of the basin in the (2010-2099) time window. While the results suggest that recent water-related challenges in the basin might have caused by climate change, further in-depth studies are required to reveal the exact reasons.

1. Introduction

Nowadays, the climate change phenomenon, due to its explicit and implicit social and political implications, has become a crucial, yet controversial, topic in the scientific community [8]. Accordingly, the United Nations Framework Convention on Climate Change (UNFCCC) defines climate change as "a change of climate which is attributed directly or indirectly to human activity that alters the composition of the global atmosphere and which is in addition to natural climate variability observed over comparable time periods." [9].

Although the main outcome of the projected changes in the climatic patterns is a rise in the global average temperature (*i.e.*, global warming), as far as the regional scale climate is of concern, any changes in the amount and/or pattern of solar energy received by the Earth can cause a systematic change in the spatial and temporal behavioral pattern of other climatic parameters. Allegedly, these changes in climate patterns are responsible for explaining some out of the ordinary events such as shifts in forest structure [11], adverse impacts on mental health [6], or even, a decline in songbird population [3].

Hydrologists and water resources managers, howev-

**Corresponding Author:*
Babak Zolghadr-Asli,
Teaching Assistant, Dept. of Irrigation & Reclamation Engineering, Faculty of Agricultural Engineering & Technology, College of Agriculture & Natural Resources, Univ. of Tehran, 3158777871 Karaj, Iran;
Email: zolghadrbabak@ut.ac.ir

DOI: https://doi.org/10.30564/hsme.v2i1.1507

er, aim to understand the impact of these changes on the water resources' status. The key to unfold the mystery behind this connection is the hydrological cycle [15]. Due to the projected changes in the pattern of the received solar energy, the global precipitation patterns may inevitably change as well. These newly emerged patterns would differ from the previously observed ones in terms of frequency, magnitude, and their temporal and spatial distribution [19]. These pieces of information then can be used as inputs to the appropriate climate models [*i.e.*, global circulation models (GCMs)] to project the climate change conditions [20]. Given that these simulations would take place on an uncharted and unprecedented territory of an uncertain future, the most logical approach to extract the global temperature and precipitation behaviors is to develop a series of climate scenarios that, in essence, should provide a range of plausible time series for the amount of radiative forces (RFs). This has been one of the main goals of the Intergovernmental Panel on Climate Change (IPCC) in the past couple of decades. IPCC's recent studies and reports have been summarized in the 5th assessment reports (AR5) [9].

Perhaps, one of the advantages of invoking these approaches to study the impact of climate change is that it can facilitate the assessment of water and environmental resources under a range of possible conditions. Although hydrologic challenges raised due to the climate change phenomenon can take many forms (*e.g.*, prolonged drought condition [18] or perhaps extreme flood events [14]), the common perception here is that these changes may exacerbate the situation of water resources in arid and semi-arid regions, such as the Middle East [16].

Water-related challenges are, by nature, multi-dimensional problems [15]. Thus, they can potentially affect social, economic, political, and environmental aspects of any given society. A real-world example of this notion, which has recently emerged in a spectacular way, is the Maharlou Lake Basin, south of Iran. Reportedly, it is the latest case of the inland water-bodies in Iran that have reached a critical water level. Ever since its near desiccation during summer 2002, Maharlou Lake, which was once considered a nearly permanent lake, has experienced seasonal drying on regular bases [4]. The role of this lake in maintaining the biodiversity in the nearby wetlands, and its economic role as a source for mineral material such as salt, necessitate a prompt and thorough investigation. The primary goal of this study is to provide a glance of likely impacts of climate change on the Maharlou Lake basin. Using CanESM2 and 5th generation of IPCC scenarios, which revolve around the concept of representative concentration pathways (RCPs), a range of possible climatic behavior will be generated. Then, the response of the basin's streamflow would be simulated using a hydrologic model, namely IHACRES. Finally, to shed light on the impact of the climate change phenomenon, the changing patterns of precipitation, temperature and streamflow parameters would be analyzed throughout the basin.

2. Methodology

This section discusses the twofold procedure required for generating climatic scenarios and then transforming them into hydrological datasets. The main steps of the applied methods are shown in Figure 1.

2.1 Generation of Climate Change Scenarios

Generating climate scenarios is a threefold procedure. The first step is to introduce a set of assumptions regarding the future performance of climatic drivers. A new concept, namely RCPs, has been proposed for exploring uncertainties from anthropogenic climate drivers in recent studies. RCPs are newly defined scenarios that specify the concentrations of greenhouse gases and their plausible emission patterns. However, unlike the previous IPCC's emission scenarios, they are not directly centered around socio-economic storylines. Instead, they are based on a different approach that includes more consistent short-lived gases and land-use changes [9]. RCP-based scenarios are identified by the approximate values of their radiative forcing (RF) (W/m^2). Using this concept, IPCC's 5th assessment reports (AR5), defined RCP 2.6, RCP 4.5, RCP 6.0, and RCP 8.5 as the new generation of climate change scenarios. Accordingly, RCP 2.6, which represents the most optimistic projection compared to the four most common RCPs, peaks at 3.0 W/m^2 and then declines to 2.6 W/m^2 by the year 2100. RCP 4.5 and RCP 6.0, which represent moderate projections for upcoming changes in the climate, stabilize after 2100 at 4.2 and 6.0 W/m^2, respectively; while RCP 8.5, which is the most pessimistic climate change projection, reaches 8.3 W/m^2 in 2100 on a rising trajectory [9]. Ultimately, the primary objective of these scenarios is to provide the input data necessary to run a comprehensive climate model. Note that due to the substantial uncertainties in RF trajectories, these forcing values represent comparative *markers*, rather than the *exact* forcing values. For more information on the definition and assumptions of these scenarios, readers can refer to van Vuuren *et al.* [17] and Zolghadr-Asli [19].

The second step for generating the climate change scenarios is to simulate the global climatic behavior in response to the assumed RCPs using a GCM, in this case, CanESM2. CanESM2 integrates an atmosphere-ocean

 DOI: https://doi.org/10.30564/hsme.v2i1.1507

general circulation model, a land-vegetation model, and five terrestrial and oceanic interactive carbon cycles. This GCM uses a Gaussian 128×64 grid to simulate the earth's climatic behavior. Accordingly, the resolution of this model is (2.8°, 2.8°) (longitude, latitude) for the atmosphere, and (1.4°, 1.4°) (longitude, latitude) for the ocean [5]. Numerous studies have validated the performance of CanESM2. Chylek *et al.* [5], for instance, reviewed the application of this GCM and shed light on the model's capacity for climatic simulation on a global scale. Accordingly, the followings factors have been identified as the key reasons for the model's superior simulations: More realistic treatment of atmospheric aerosols [12], surface use changes [13], and introduction of clouds in the simulation process [7]. See Chylek *et al.* [5] and Zolghadr-Asli *et al.* [20] for more details.

Given that GCM projections use large-scale computational grids, the generated results for most regional study areas could not be considered adequately accurate. Consequently, the final step is spatial downscaling of the GCM outputs via methods such as the change factor technique. In this simple weather typing approach, the climate scenarios are obtained by computing the differences (or ratio, depending on the nature of the climate variables) between the averages of the GCM dataset for the climate change period and the corresponding averages of the model's simulation results for the baseline period. The above-mentioned spatial downscaling procedure can be mathematically expressed as follows [2]:

$$\Delta T_i = \overline{T}_i^{fut} - \overline{T}_i^{base} \tag{1}$$

$$\Delta P_i = \frac{\overline{P}_i^{fut}}{\overline{P}_i^{base}} \tag{2}$$

$$T_i = T_i^{obs} + \Delta T_i \tag{3}$$

$$P_i = P_i^{obs} \times \Delta P_i \tag{4}$$

in which ΔT_i and ΔP_i are the expected changes in the long-term monthly average of temperature and rainfall for the ith month, respectively. $\overline{T}_i^{fut}$ and $\overline{P}_i^{fut}$ represent the long-term monthly average of temperature and rainfall for month *i* simulated by the GCM for the climate change period, respectively. $\overline{T}_i^{base}$ and $\overline{P}_i^{base}$ denote the long-term monthly average of temperature and rainfall for month *i* simulated by the GCM for the baseline period, respectively. T_i^{obs} and P_i^{obs} represent the observed temperature and rainfall for month *i*, respectively. Finally, T_i and P_i are the temperature and rainfall for month i in the climate change period, respectively. For further information on this technique, refer to Adhikari *et al.* [2] and Zolghadr-Asli *et al.* [21].

2.2 Hydrological Simulations

The last step, *i.e.*, hydrologic simulation, transforms the generated climatic scenarios into the hydrologic responses. IHACRES (identification of unit hydrographs and component flows from rainfall, evaporation, and streamflow data) is a lumped, semi-conceptual model [10], which has been proven to be a practical option for such a task. IHACRES is composed of two modules: A non-linear loss module, which converts the observed rainfall into the effective rainfall, and a linear unit hydrograph module, which converts the estimated effective rainfall into the simulated streamflow. One of the major advantages of IHACRES over other commonly used rainfall-runoff models is its minimal input data requirement (*i.e.*, temperature and rainfall) [21]. For further information on this model, the readers can refer to Abushandi & Merkel [1].

Naturally, the IHACRES model needs to be calibrated and validated. The three quantitative statistical parameters used to evaluate the performances of the IHACRES model include Nash-Sutcliffe efficiency (*NSE*) coefficient, percent bias (*PB*), and the ratio of root-mean-square error (*RMSE*) to observations standard deviation ratio (*RSR*), which are respectively given by [2]:

$$NSE = 1 - \left[\frac{\sum_{t=1}^{N} (x_t^{obs} - x_t^{sim})}{\sum_{t=1}^{N} (x_t^{obs} - x_{mean}^{obs})} \right]^2 \tag{5}$$

$$PB = \left[\frac{\sum_{t=1}^{N} (x_t^{obs} - x_t^{sim})}{\sum_{t=1}^{N} x_t^{obs}} \right] \times 100 \tag{6}$$

$$RSR = \left[\frac{\sqrt{\sum_{t=1}^{N} (x_t^{obs} - x_t^{sim})^2}}{\sqrt{\sum_{t=1}^{N} (x_t^{obs} - x_{mean}^{obs})^2}} \right] \tag{7}$$

where x_t^{obs} and x_t^{sim} are observed and simulated streamflow in the *t*th time step, respectively; x_{mean}^{obs} is mean of the observed streamflow data; and *N* is the num-

DOI: https://doi.org/10.30564/hsme.v2i1.1507

ber of time steps. *NSE* ranges from $-\infty$ to 1.0 (1.0 for a perfect fit), and *RSR* ranges from 0 to $+\infty$ (0 for a perfect fit). For a monthly time step, a *PB* value between −25 and +25%, an *NSE* value greater than 0.5, or an RSR value less than or equal to 0.7 is considered satisfactory.

3. Study Area

The Maharlou lake basin (Figure 2), with a catchment area of 4,720 km^2, is located in the south-western region of Iran (latitude: 29 - 30° N; longitude: 52 - 53° E). While the basin experiences mild spatiotemporal variations in rainfall, the temperature shows little spatial variation throughout the basin. The southern part of the basin receives an average annual rainfall of approximately 250 mm, while in the northern and middle parts of the basin, the average annual rainfall is as high as 480 mm. The average annual rainfall of the basin is 390 mm. Figure 3 illustrates the average annual rainfall in the period (1987-2016). The average annual temperature in this area ranges from 18 to 19 °C, with the regional average of approximately 19 °C. Figure 4 demonstrates the average annual temperature within the period (1987-2016). Due to the basin's semi-arid climate, the streams are seasonal and only within the wet seasons have notable water flows. Figure 5 shows the average annual streamflow in the baseline period (1975-2016).

4. Results & Discussion

In order to evaluate the range of climate change outcomes on the Maharlou Lake basin, the CanESM2 model was used to simulate rainfall and temperature for the RCP 2.6, RCP 4.5, and RCP 8.5 scenarios for the baseline period of 1987 to 2016. Figures 6 and 7 demonstrate the basin's monthly average rainfall and temperature during the baseline period, respectively. The main assumption of *change factor* downscaling technique is to assume that the amount of changes in the regional hydro-climatic variables is equivalent to the amount of computed differences between GCM's simulations under climate change and baseline conditions. In other words, change factor represents the amount of change in each parameter under the projected climate change condition. In this study, the duration of climate change period was divided into three time-frames: (a) near-future (2010-2039), (b) mid-future (2040-2069), and (c) far-future (2070-2099). Next, the large-scale outputs of the CanESM2 model were downscaled using the change factor technique [Equations (1) to (4)]. Figures 8 and 9, for instance, illustrate the change factors that can be expected for monthly rainfall and temperature for the near feature, under RCP 2.6 assumptions, respectively. Furthermore, the monthly average of rainfall and temperature under both baseline and climate change conditions in January are summarized in Table 1 and 2, respectively. Overall, the results showed that under RCP 2.6, RCP 4.5, and RCP 8.5 scenarios, the average annual rainfall of 350, 363, and 387 mm in the near-future; 377, 355, and 394 mm in the mid-future; And 369, 366, and 400 mm in the far-future, can be expected, respectively. Given the annual average rainfall of 389 mm, in all likelihood, the average rainfall in the basin would drop by 6% and 7% under RCP 2.6 and RCP 4.5 conditions, respectively, while under RCP 8.5 scenario, it might be raised by 1%. Additionally, under RCP 2.6, RCP 4.5, and RCP 8.5 conditions, the average annual temperature was estimated to be 19.24, 19.18, and 19.21 °C for near-feature, and 19.29, 19.33, and 19.45 °C for mid-future, and 19.29, 19.40, and 19.69 °C for far-future, respectively. Given that the average annual temperature in the baseline is 18.90 °C, one can expect a 2%, 2%, and 3% raise under RCP 2.6, RCP 4.5 and RCP 8.5 scenarios, respectively.

The next step would be to anticipate the basin's hydrologic responses to the climate change conditions in a monthly time step using IHACRES model. The model was calibrated separately for the basin's main rivers, that are Rahdar river (Chenar station), Khoshk river (Chenar-Sookhteh station), and Baba-Haji river (Pol-e-Fasa station) using a monthly time step. The observed and simulated streamflow of the above-mentioned rivers are illustrated in Figures 10. Furthermore, the quantitative statistical parameters for evaluating the calibration and validation procedure are listed in Table 3. As can be seen, all the quantitative statistical parameters (*i.e.*, *NSE, PB, RMSE*) indicate that the generated models can represent the hydrologic conditions of the above-mentioned rivers.

The final step would be to utilize the developed models to simulate the basin's hydrological response to climate change conditions. The result of these simulations during the (2010-2039) time-frame, for instance, has been summarized in Figures 11 to 13. Similarly, the results of these simulations were analyzed using their monthly average values. Table 4, for instance, summarized the monthly average discharge of the basin's main rivers under both baseline and climate change conditions in January. Overall, the average streamflow would be 0.76, 0.82, and 0.93 m^3/s under RCP 2.6, RCP 4.5, and RCP 8.5 scenarios for near-future, 0.89, 0.78, and 0.98 m^3/s for mid-future, and 0.85, 0.84, and 1.02 m^3/s for far-future, respectively. Given that the average annual streamflow of the basin is 1.15 m^3/s, one can conclude that the average streamflow of the basin would face a 28%, 30%, and 15% drop under RCP 2.6, RCP 4.5 and RCP 8.5 scenarios, respectively.

 DOI: https://doi.org/10.30564/hsme.v2i1.1507

5. Concluding Remarks

There is little doubt on the fact that the general climatic behavior of our planet is going to change. These changes, along with the world's population growth, are most likely to influence the next generations' future; thus, it is not unreasonable to expect higher food, water, and energy demands in the upcoming years. In the context of hydro-climatic sciences, one should bear in mind that these projected changes can affect both the demand and supply side of water resources. Thus, the first step to promote a *sustainable* future would be to predict these changes. These predictions could help the decision-makers to devise a *robust* solution to mitigate and adapt to these changes. The notion above is especially crucial in semi-arid and arid regions such as the Middle East, where the security of water resources has already been jeopardized.

With that in mind, this study aimed to evaluate the potential impacts of climate change on the Maharlou Lake basin, Iran. The results have demonstrated a 4% decrease in average annual rainfall, a 2% increase in average annual temperature, and, finally, a 24% decrease in average annual streamflow of the basin in the (2010-2099) time window. In conclusion, according to the results, climate change phenomenon, in all likelihood, might worsen the situation for the basin's water resources. An expected decrease in the basin's average rainfall and streamflow, and an increase in the temperature, may increase the pressure on the water resources of a basin that suffers from water stress. While the simulated results might help partially explain the recent changes in the Maharlou Lake basin's conditions, further in-depth studies are required to reveal the exact reason behind the observed situation, in recent past.

Declarations

Availability of Data and Material

CanESM2 output data provided by the CCCma, ECCC: http://climate-modelling.canada.ca/climatemodeldata/data.shtml; the other datasets used and/or analyzed during the current study are available from the corresponding author on reasonable request.

Competing Interests

The authors declare that they have no competing interests.

Funding

This study was not supported by any public, commercial, or not-for-profit organization, and the authors did not receive any financial support to conduct this analysis.

Author' Contributions

Both Authors participated in the data analysis process and writing the manuscript. All authors read and approved the final manuscript.

Acknowledgments

Not applicable.

Appendixes

Table 1. the monthly average of rainfall (mm) under baseline and climate change conditions in January

	Station	Baseline	(2010-2039)	(2040-2069)	(2070-2099)
RCP 2.6	Dobaneh	93	74	84	77
	Ghalat	120	94	107	98
	Mehrabad-Ramjerd	81	63	72	65
	Sarvestan	54	41	48	43
	Shiraz (Sazman-e-Ab)	89	70	80	73
RCP 4.5	Dobaneh	93	78	77	77
	Ghalat	120	99	99	99
	Mehrabad-Ramjerd	81	66	66	66
	Sarvestan	54	44	43	43
	Shiraz (Sazman-e-Ab)	89	74	73	73
RCP 8.5	Dobaneh	93	88	80	84
	Ghalat	120	112	102	108
	Mehrabad-Ramjerd	81	76	68	73
	Sarvestan	54	50	45	48
	Shiraz (Sazman-e-Ab)	89	83	76	80

Table 2. the monthly average of temperature (°C) under baseline and climate change conditions in January

	Station	Baseline	(2010-2039)	(2040-2069)	(2070-2099)
RCP 2.6	Fasa	7.18	7.61	7.62	7.62
	Sad-e-Dorodzan	5.24	5.96	5.97	5.98
	Shiraz (Synoptic)	6.14	6.64	6.65	6.65
	Zarghan	5.61	6.22	6.23	6.24
RCP 4.5	Fasa	7.18	7.48	7.65	7.72
	Sad-e-Dorodzan	5.24	5.75	6.02	6.14
	Shiraz (Synoptic)	6.14	6.49	6.69	6.77
	Zarghan	5.61	6.04	6.27	6.38
RCP 8.5	Fasa	7.18	7.56	7.74	7.93
	Sad-e-Dorodzan	5.24	5.88	6.17	6.49
	Shiraz (Synoptic)	6.14	6.58	6.79	7.02
	Zarghan	5.61	6.15	6.4	6.68

DOI: https://doi.org/10.30564/hsme.v2i1.1507

Table 3. quantitative evaluation of model calibration and validation results for the basin's main rivers

Rahdar river	**Calibration**	**Period**	**(1996-2016)**
		NSE	0.72
		PB (%)	5
		RSR	0.53
	Validation	Period	(1988-1995)
		NSE	0.68
		PB (%)	24
		RSR	0.56
Khoshk river	**Calibration**	Period	(1997-2016)
		NSE	0.64
		PB (%)	-19
		RSR	0.60
	Validation	Period	(1988-1996)
		NSE	0.77
		PB (%)	23
		RSR	0.48
Baba-Haji river	**Calibration**	Period	(1997-2016)
		NSE	0.67
		PB (%)	6
		RSR	0.57
	Validation	Period	(1988-1996)
		NSE	0.79
		PB (%)	25
		RSR	0.45

Table 4. the monthly average of streamflow (m^3/s) under baseline and climate change conditions in January

	Station	**Baseline**	**(2010-2039)**	**(2040-2069)**	**(2070-2099)**
RCP 2.6	Chenar	1.52	0.65	0.81	0.69
	Che-nar-Sookhteh	1.17	0.91	1.17	0.97
	Pol-e-Fasa	4.16	2.11	2.57	2.28
RCP 4.5	Chenar	1.52	0.71	0.65	0.67
	Che-nar-Sookhteh	1.17	0.98	0.94	0.98
	Pol-e-Fasa	4.16	2.29	2.11	2.21
RCP 8.5	Chenar	1.52	0.82	0.84	0.86
	Che-nar-Sookhteh	1.17	1.15	1.25	1.37
	Pol-e-Fasa	4.16	2.63	2.69	2.67

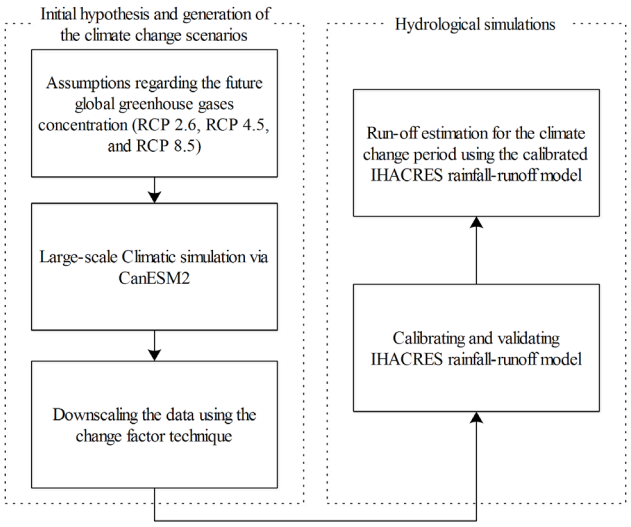

Figure 1. flowchart of the applied methodology

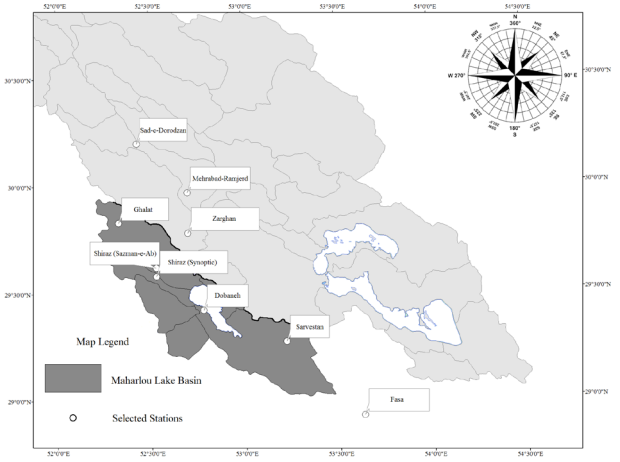

Figure 2. the location of the study area and selected stations

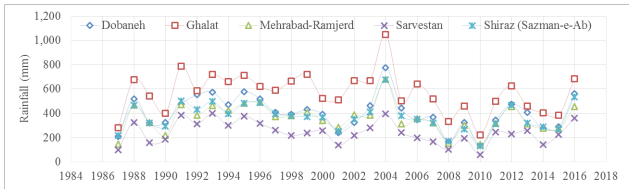

Figure 3. average annual rainfall (mm) in the baseline period (1987-2016)

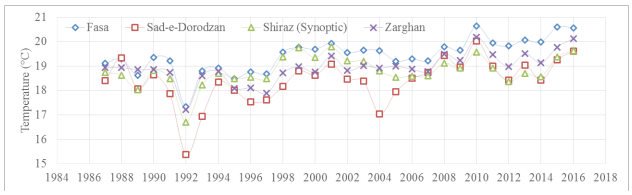

Figure 4. average annual temperature (°C) in the baseline period (1987-2016)

 DOI: https://doi.org/10.30564/hsme.v2i1.1507

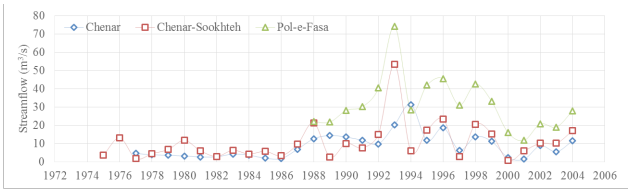

Figure 5. average annual streamflow (m^3/s) in the baline period (1975-2016)

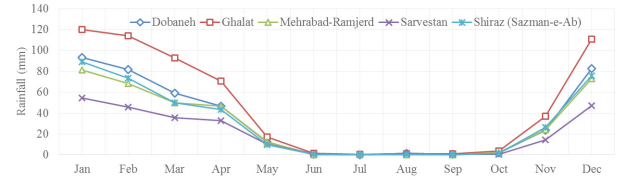

Figure 6. monthly average rainfall (mm) of the selected stations in the baseline period (1975-2016)

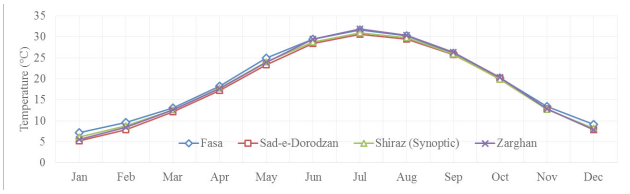

Figure 7. monthly average temperature (°C) of the selected stations in the baseline period (1975-2016)

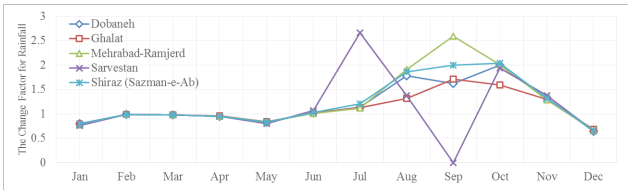

Figure 8. the change factor for rainfall (mm) under RCP 2.6 assumptions during (2010-2039)

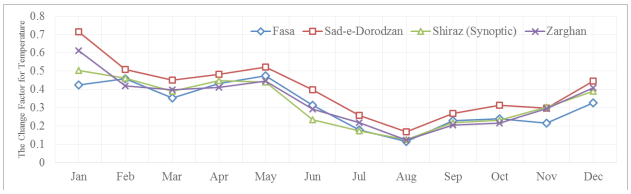

Figure 9. the change factor for temperature (°C) under RCP 2.6 assumptions during (2010-2039)

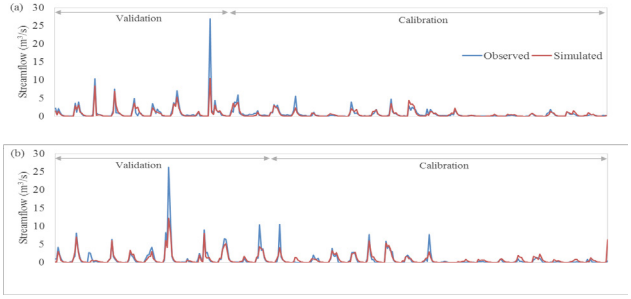

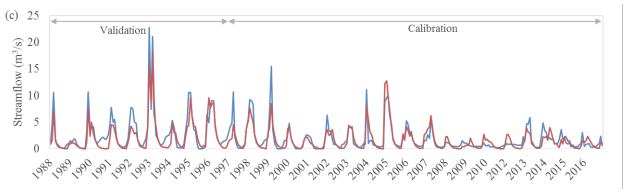

Figure 10. observed and simulated streamflow (m^3/s) on a monthly time step for: (a) Rahdar river, (b) Khoshk river, and (c) Baba-Haji river

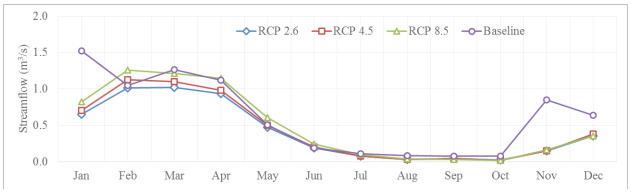

Figure 11. monthly average discharge (m^3/s) of Rahdar river during (2010-2039)

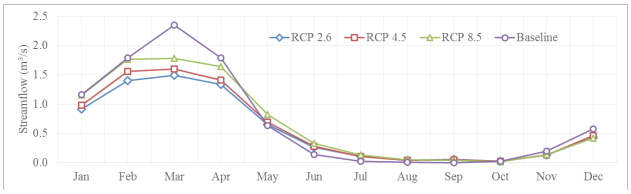

Figure 12. monthly average discharge (m^3/s) of Khosh river during (2010-2039)

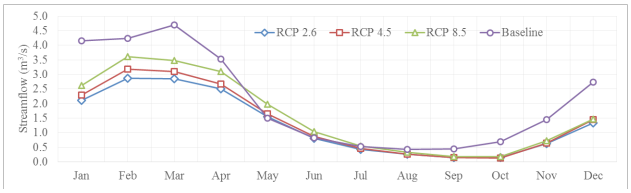

Figure 13. monthly average discharge (m^3/s) of Baba-Haji river during (2010-2039)

References

[1] Abushandi, E. & Merkel, B. Modelling rainfall runoff relations using HEC-HMS and IHACRES for a single rain event in an arid region of Jordan. Water Resources Management, 2013, 27(7): 2391-2409.

[2] Adhikari, U., Nejadhashemi, A.P., Herman, M.R. & Messina, J.P.. Multiscale assessment of the impacts of climate change on water resources in Tanzania. Journal of Hydrologic Engineering, 2016, 22(2): 05016034.

[3] Bonnot, T.W., Cox, W.A., Thompson, F.R. & Millspaugh, J.J.. Threat of climate change on a songbird population through its impacts on breeding. Nature Climate Change, 2018, 8(8): 718.

[4] Brisset, E., Djamali, M., Bard, E., Borschneck, D.,

DOI: https://doi.org/10.30564/hsme.v2i1.1507

Gandouin, E., Garcia, M., Stevens, L. & Tachikawa, K.. Late Holocene hydrology of Lake Maharlou, southwest Iran, inferred from high-resolution sedimentological and geochemical analyses. Journal of Paleolimnology, 2018, 61(1): 1-18.

[5] Chylek, P., Li, J., Dubey, M.K., Wang, M. & Lesins, G.. Observed and model simulated 20th century Arctic temperature variability: Canadian earth system model CanESM2. Atmospheric Chemistry and Physics Discussions, , 2011, 11(8): 22893-22907.

[6] Cunsolo, A. & Ellis, N.R.. Ecological grief as a mental health response to climate change-related loss. Nature Climate Change, 2018, 8(4): 275.

[7] Dijkstra, H.A., Te Raa, L., Schmeits, M., & Gerrits, J.. On the physics of the Atlantic multidecadal oscillation. Ocean Dynamics, 2006, 56(1): 36-50.

[8] Gleick, P.H. Water strategies for the next administration. Science, 2016, 354(6312): 555-556.

[9] IPCC. "Climate change 2013: The physical science basis." Contribution of Working Group I to the Fifth Assessment Report of the Intergovernmental Panel on Climate Change, Cambridge University Press, Cambridge, United Kingdom and New York, NY, 2013.

[10] Jakeman, A.J. & Hornberger, G.M.. How much complexity is warranted in a rainfall-runoff model? Water Resources Research, 1993, 29(8): 2637-2649.

[11] Lesk, C., Coffel, E., D'Amato, A.W., Dodds, K. & Horton, R.. Threats to North American forests from southern pine beetle with warming winters. Nature Climate Change, 2017, 7(10): 713.

[12] Mishchenko, M.I., Liu, L., Geogdzhayev, I.V., Travis, L.D., Cairns, B., & Lacis, A.A.. Toward unified satellite climatology of aerosol properties: MODIS versus MISR versus AERONET. Journal of Quantitative Spectroscopy & Radiative Transfer, 2010, 111(4): 540-552.

[13] Pielke, R.A., Adegoke, J., Beltrán-Przekurat, A., Hiemstra, C.A., Lin, J., Nair, U.S., Niyogi, D., & Nobis, T.E.. An overview of regional land-use and land-cover impacts on rainfall. Tellus: Physical & Chemical Meteorology, 2007, 59(3): 587-601.

[14] Ryu, Y., Kim, Y.O., Seo, S.B., & Seo, I.W.. Application of real option analysis for planning under climate change uncertainty: A case study for evaluation of flood mitigation plans in Korea. Mitigation and Adaptation Strategies for Global Change, 2018, 23(6): 803-819.

[15] Singh, V.P., Khedun, C.P. & Mishra, A.K.. Water, environment, energy, and population growth: Implications for water sustainability under climate change. Journal of Hydrologic Engineering, 2014, 19(4): 667-673.

[16] Sowers, J., Vengosh, A. & Weinthal, E.. Climate change, water resources, and the politics of adaptation in the Middle East and North Africa. Climate Change, 2011, 104(3): 599–627.

[17] Van Vuuren, D.P., Edmonds, J., Kainuma, M., Riahi, K., Thomson, A., Hibbard, K., Hurtt, G.C., Kram, T., Krey, V., Lamarque, J.F. & Masui, T.. The representative concentration pathways: An overview. Climatic Change,, 2011, 109(1-2): 5.

[18] Wang, Z., Zhong, R., Lai, C., Zeng, Z., Lian, Y., & Bai, X.. Climate change enhances the severity and variability of drought in the Pearl River Basin in South China in the 21st century. Agricultural and Forest Meteorology, 2018, 249: 149-162.

[19] Zolghadr-Asli, B.. Discussion of "Multiscale Assessment of the Impacts of Climate Change on Water Resources in Tanzania" by Umesh Adhikari, A. Pouyan Nejadhashemi, Matthew R. Herman, and Joseph P. Messina. Journal of Hydrologic Engineering, 2017, 22(8): 07017010.

[20] Zolghadr-Asli, B., Bozorg-Haddad, O. Sarzaeim, P., & Chu, X.. Investigating the variability of GCMs' simulations using time series analysis. Journal of Water and Climate Change, 2018a.
DOI: 10.2166/wcc.2018.099

[21] Zolghadr-Asli, B., Bozorg-Haddad, O. & Chu, X.. Effects of the uncertainties of climate change on the performance of hydropower systems. Journal of Water and Climate Change, 2018b.
DOI:10.2166/wcc.2018.120

 DOI: https://doi.org/10.30564/hsme.v2i1.1507